

Near-terminator Martian ionosphere during sunspot cycle 23 from Mars Global Surveyor radio science measurements

Ashok Kumar, Neelesh K Lodhi & K K Mahajan

Radio and Atmospheric Sciences Division, National Physical Laboratory, New Delhi 110 012, India

Received 31 July 2007; accepted 28 September 2007

Radio Science experiment on the Mars Global Surveyor (MGS) has measured a large number of electron density profiles in the near-terminator Martian ionosphere, from December 1998 to March 2005, thus covering rising, maximum and declining phase of sunspot cycle 23. More than a dozen data sets, EDS 1 to EDS 13, are now available at the public website and these sets contain profiles numbering from a few tens in some sets to several hundreds in others. On any one day, several profiles were measured at a constant solar zenith angle (χ) but at different longitudes. However, χ varied considerably during each data set and in this paper about 2000 profiles have been analysed to study the height (h_m) and density (N_m) of the primary peak as a function of solar zenith angle. A significant decrease of N_m is seen with increasing χ , but h_m starts increasing at χ above 80° only. To examine how close the Martian primary peak is to an ideal Chapman layer, values of exponent, k and sub-solar peak density, N_o in the equation $N_m = N_o (\cos \chi)^k$ were obtained by using the largest number of profiles employed ever before. A value of 0.45 for the exponent k deduced is somewhat smaller than the value of 0.5 expected for an ideal Chapman layer. Value of N_o was found to be $1.75 \times 10^{11} \text{ m}^{-3}$. Anomalous features in the Mars ionosphere seen in the earlier MGS data are found to be present in the latest data also.

Keywords: Martian ionosphere, Mars Global Surveyor (MGS), Chapman layer, Electron density profiles, Solar zenith angle

PACS No.: 96.35.Kx

1 Introduction

Radio science (also called radio occultation) experiments aboard several space missions have measured a large number of electron density profiles in the Martian ionosphere. In this technique (see e.g. Kliore *et al.*¹) a radio signal at a few cm wavelength is transmitted by the spacecraft to Earth and as it enters behind or comes out from the far side of the planet, the signal is modulated by the neutral atmosphere and ionosphere. There is a Doppler shift in the frequency of the signal received, which is then used to derive vertical electron density profile. This technique on the space mission Mariners-4 gave the first indication of a substantial ionosphere at Mars and measured^{1,2} a dayside peak value (N_m) of 10^{11} m^{-3} at an altitude (h_m) of about 125 km. This mission was during a period of low solar activity. Radio occultation measurements were repeated on Mariner-6 and -7, which were during a period of high solar activity³. These early missions were fly byes, thus only two profiles, one on entry and the other on exit from the ionosphere, could be measured.

The real advance in exploring Mars ionosphere was made by Mariner-9, which was an orbiter. Several electron density profiles in the altitude range 100-300

km were measured by Kliore *et al.*^{4,5} during the primary and the extended mission, which were during a period of moderate solar activity. Electron density profiles in the Martian ionosphere were also measured by Kolosov *et al.*⁶ on the Soviet spacecraft Mars-2 during a moderate solar activity period. The American mission Mariner-9 was followed by Viking-1 and -2, which had both landers and orbiters. The orbiters had radio science experiment, while each lander had a retarding potential analyzer, which provided a direct measurement of the concentration of electrons as well as of individual ions⁷. This was the first *in situ* ionospheric measurement at a planet other than the Earth. Viking-1 and -2 made these measurements during a period of very low solar activity.

During a span of about 15 years, from 1965 to 1980, only a total of 443 electron density profiles were recorded by radio science experiments on various US and Soviet space missions at various levels of solar activity and at different sun spot cycles⁸. These measurements thus provided a broad structure of Mars ionosphere⁹⁻¹¹. But more recently the Mars Global Surveyor (MGS)^{12,13} measured several thousand electron density profiles from December 1998 to March 2005, thus providing a large

data base for studying the fine structure of Martian ionosphere during various phases of sunspot cycle 23. These profiles are available at <ftp://pds-geosciences.wustl.edu/mgs-m-rss-5-sdp-v1>, courtesy of Hinson¹². Although each profile observed by MGS is confined within the altitude range 100-200 km, it contains more than 95% of the ionospheric electron content and thus is capable of providing all the desired information regarding Mars aeronomy. A new feature of the MGS radio science measurements was that several profiles were recorded on any single day at the same solar zenith angle (χ), but at different longitudes. Thus the MGS radio science profiles provided a unique opportunity, not only to study the solar activity and SZA related changes, but the longitudinal variations also. In the sections that follow the authors shall first summarize some important results recently reported from the MGS radio science profiles, then give a brief account of the data analysed by them in this paper and finally present their results on Mars ionosphere by using the largest number of electron density profiles ever used before.

2 Some recent results on Mars ionosphere from MGS radio science data

In the recent past MGS-electron density profiles have been used by a number of workers to study several important features of Martian ionosphere. Bougher *et al.*¹⁴ were the first to analyze the initial set of 32-profiles for the period 24-31 Dec. 1998 and found a longitudinal dependence of height of the primary peak h_m . These profiles sampled high northern latitudes (64.7-67.3 °N), at local times from 0300 to 0400 hrs LT and at SZAs from 78 to 81°. Thus these measurements were essentially limited to a single latitude, solar local time and solar zenith angle. Realizing that under these circumstances for a photochemical layer, h_m should have remained constant for all these 32 profiles, Bougher *et al.*, attributed this longitudinal variation to changes in the neutral atmosphere. They plotted h_m as function of longitude and discovered oscillation of wave number up to 3 in the Martian ionosphere. These authors further found that this feature also existed in the neutral density at 130 km, measured by the MGS accelerometer experiment¹⁵. This result thus linked the Mars ionospheric dynamics to the underlying neutral atmosphere. Bougher *et al.*¹⁶ subsequently analyzed MGS-radio science data for two Martian years and concluded wave number 2-3 oscillations in the Mars ionosphere from the h_m data. Mahajan *et al.*¹⁷, using

the same data sets as employed by Bougher *et al.*¹⁶, found that not only h_m but N_m also exhibited the same kind of variability for profiles recorded on the same day and at the same solar zenith angle. These authors further found longitudinal patterns in N_m also, which were somewhat similar to these seen by Bougher *et al.*^{14,16}, but with some phase delays.

Martinis *et al.*¹⁸ examined the effect of solar irradiance on the Mars electron density profiles by using a photochemical model and compared these with the MGS observations for the period 9-27 Mar. 1999. They found that their photochemical model, very adequately agreed with observations. Similarly Mendillo *et al.*¹⁹ compared the peak values of electron density observed at Mars by the MGS, with the same day values of E-layer peak density on Earth for the same period (viz. 9-27 Mar. 1999), as studied by Martinis *et al.*¹⁸ and found a good agreement in scaling laws between the two planets. Rishbeth and Mendillo²⁰ by comparing electron density of the ionospheric layers E and F1 at Mars (which they named as M1 and M2, respectively) with those observed at Earth, concluded that day-to-day variations in electron density at Mars as well as at Earth are basically caused by changes in solar activity. They identified features of M1-layer at Mars with those of E-layer at Earth and that of M2-layer at Mars with those of F1-layer at Earth.

Krymskii *et al.*²¹ combined the MGS measurements of the radio science experiment with the Magnetometer/Electron Reflectometer experiment²² and studied the effect of crustal magnetic fields on the near terminator ionosphere of Mars. They found that since the crustal magnetic fields are weak in the northern hemisphere, the solar wind interacts directly with the ionosphere in the northern hemisphere. However, in some limited regions in the southern hemisphere, where the crustal magnetic fields are strong, large scale mini-magnetospheres are formed. By studying scale heights of electron density profiles (137 in the northern hemisphere and 219 in the southern hemisphere), they concluded that neutral atmosphere is cooler and electrons hotter inside these large scale mini-magnetospheres. Krymskii *et al.*²³, in a subsequent work and with more extended electron density profiles data (907 profiles in the northern hemisphere and 219 profiles in the southern hemisphere), compared the solar wind interaction in the two hemispheres and concluded that ionospheric parameters show larger variability in the southern

hemisphere than in the northern hemisphere. This they ascribed mostly to variability of magnetic field direction from local zenith. Breus *et al.*²⁴, employing the same radio science electron density profiles data as used by Krymskii *et al.*²³, studied the effect of solar radiation in the topside atmosphere/ionosphere of Mars. They found that the peak electron density was heavily dependent on solar zenith angle in the near terminator ionosphere. They further found that peak electron density, N_m , was higher in the southern hemisphere than in the northern hemisphere and concluded from aeronomic considerations, that the electron temperature would be higher in the southern hemisphere as compared to that in the northern hemisphere. A similar attempt to study the effect of solar radiation on the peak density of the Martian ionosphere was made by Zou *et al.*²⁵ who examined MGS electron density profiles for two very extended periods – one from November 2000 to June 2001 and the other from October 2002 to June 2003 and found a good response of N_m to the EUV flux index, E10.7 of Tobiska *et al.*²⁶ on short term, as well as long term basis. They too concluded higher electron temperature in the strong magnetic field regions in the southern hemisphere, as compared to those in the non-magnetic-field region in the northern hemisphere.

In addition to above investigations, wave-like structures have also been detected in the topside ionosphere of Mars from the MGS radio science profiles by Wang and Nielsen²⁷. Effects of some episodic events like solar flares have been observed by Mendillo *et al.*⁸, who noted enhancements up to 200 % in the Mars lower ionosphere during the April 2001 solar flares. They concluded these to be due to relatively larger enhancements in the soft X-ray fluxes than those in the UV. Mahajan *et al.*¹⁷ identified some anomalous features in the MGS radio science profiles. They observed significant variability in the height and density of the primary peak on the same day, for the same solar zenith angle – features not expected for a photochemical layer. With the availability of more MGS electron density profiles, the Martian ionosphere is re-visited in this paper to examine the SZA and solar activity control, as well as to ascertain whether the anomalous features reported by Mahajan *et al.*¹⁷, exist in the latest data sets also.

3 MGS radio science electron density data analyzed

As mentioned earlier, MGS radio science experiment has generated a very comprehensive set of

electron density profiles during the period December 1998 to March 2005. These profiles are in the form of 13 data sets, (EDS 1 - EDS 13), each data set containing varying number of profiles, with as little as 32 profiles for one of the data sets (EDS 1) and as many as 840 profiles for another (EDS 7). Figure 1 shows a few selected electron density profiles observed by the MGS at Mars, demonstrating average behaviour at various SZAs, although a lot of variability exists even for profiles observed on the same day for the same SZA¹⁷. Most of the profiles in Fig. 1 exhibit two peaks; an upper peak which appears in the range 120-160 km and a lower peak which appears in the range 105-140 km. The altitude and density of these peaks, generally, depend upon SZA. Electron density of the upper peak is somewhat stable and on an average dependent on solar conditions (i.e. SZA, EUV flux). This peak is now known to be formed by photo ionization of CO₂ by UV photons with wavelength of 15-100 nm. The CO₂⁺ ions produced, after some charge exchange processes with O and then with CO₂, eventually result in an ionosphere, which is dominated by O₂⁺ ions. The lower layer is formed due to absorption of solar soft X-ray photons, followed by ionization by the high energy photo-electron and the secondary electrons generated during the process. Since soft X-rays are highly variable, the electron density in this layer varies vastly^{26,28}. Most of the studies on Mars ionosphere, therefore have concentrated on the upper peak, which is now known to be called as F1 peak²⁹. This paper too deals with studies of the F1 peak only.

4 Analysis and results

The MGS electron density profiles have been sampled during various phases of sunspot cycle 23

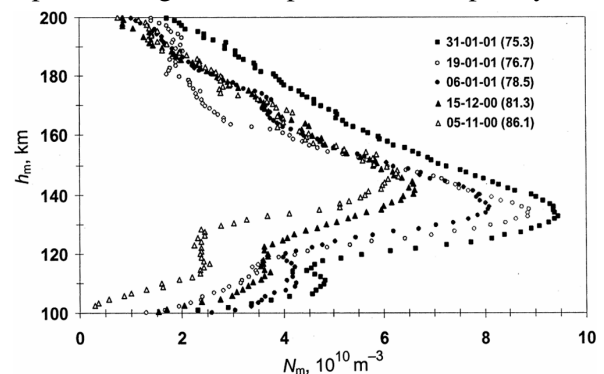


Fig. 1—A few selected electron density profiles measured by the radio science experiment on the Mars Global Surveyor demonstrating the average features [Number in parenthesis is the solar zenith angle for the profile concerned.]

and the solar activity varied considerably during this cycle. The solar EUV flux, which is the major source for the formation of Martian F1 layer, varies on short term as well as on long term basis. The short term variations are due to the solar rotation while long term variations are due to the 11-year sunspot cycle. Figure 2 shows the solar EUV flux integrated over the wavelength region 26-34 nm for the period 01 Jan. 1996 to 31 Dec. 2006 as measured by the Solar EUV Monitor (SEM) instrument on the Solar Heliospheric Observatory SOHO³⁰. These data are available on SOHO's website: ftp://pds-geosciences.wustl.edu/mgs-m-rss-5-sdp-v1. The periods for which the MGS electron density profiles (data sets EDS 1, EDS 2, EDS 5, EDS 6, EDS 8 and EDS 9) have been analysed in this paper are marked on the time scale in Figure 2. These data are listed in Table 1 along with other relevant information regarding dates, number of profiles, SZA and latitude. Since EDS 3 is a subset of EDS 5, it is not listed in Table 1. Electron density profiles in these data sets are from northern hemisphere and thus are relatively free from the effects of crustal magnetic field. The data set EDS 4

has not been used in this analysis, because this data set is for southern latitudes, where crustal magnetic fields could play a dominant role in the aeronomy of the Martian ionosphere²⁴. One can note from Fig. 1 that EDS 1 and EDS 2 are near the rising phase, EDS 5 and EDS 6 near the maximum phase and EDS 8 and EDS 9 during the declining phase of the sunspot cycle 23. However a quick look at the EUV flux data indicates that solar activity was moderate during EDS 1, 2 and 9, moderately high during EDS 8 and quite high during EDS 5 and 6 with average EUV flux of 2.25×10^{10} , 2.5×10^{10} and 2.75×10^{10} photons $\text{cm}^{-2} \text{s}^{-1}$, respectively for these periods.

4.1 Solar zenith angle dependence

The MGS radio science electron density profiles analysed by the authors are for solar zenith angles, which are quite close to the terminator. For a photochemical layer, steep changes in electron density profiles are expected to occur for such profiles. Figures 3(a)-(c) show plots of the density (N_m) and height (h_m) of the primary peak as function of solar zenith angle (χ) for the data sets, (a) EDS 1, 2, 9 (b) EDS 8 and (c) EDS 5, 6. One can note a rapid decrease in N_m as χ increases from 73° to 87° . However there is little change in N_m with SZA between 71° to 73° . Similarly there is no appreciable change in the height of the peak for SZAs less than 80° . For SZAs more than 80° , h_m rises sharply. Figure 3(d) shows mass plots of h_m and N_m against SZA. A median or mean drawn through the data points will very adequately represent the behaviour of peak parameters N_m and h_m with SZA for moderately high solar activity.

4.2 How close to ideal Chapman layer

Mars ionosphere is generally assumed to be in a photochemical equilibrium and can be described by a Chapman layer, where the peak electron density N_m is related to the solar zenith angle by the following equation

$$N_m = N_o (\cos \chi)^{0.5} \dots (1)$$

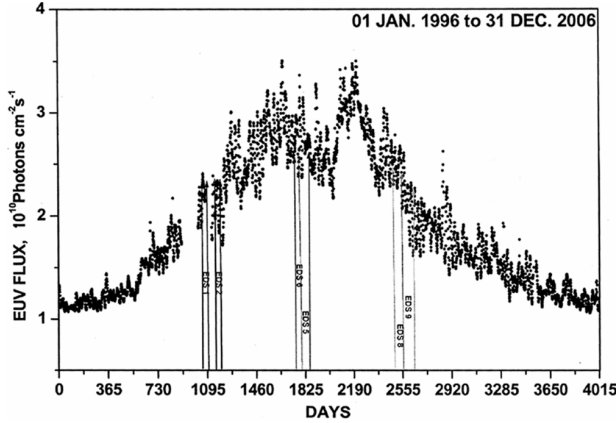


Fig. 2—Integrated solar EUV flux in the range 26-34 nm as measured by Solar Heliospheric Observatory during the period from 01 Jan. 1996 to 31 Dec. 2006 [The periods for which MGS radio science data sets EDS 1, 2, 5, 6, 8 and 9, analyzed in this paper, are also indicated (01 day on X-axis is 01 Jan. 1996.)]

Table 1—MGS radio science electron density data sets analysed

Data Set	Period	Number of profiles	SZA	Latitude
EDS 1	24-31 Dec. 1998	32	78.4-80.8	64.7-67.2
EDS 2	09-27 Mar. 1999	43	76.4-77.8	69.7-73.3
EDS 5	09 Dec. 2000 - 31 Jan. 2001	448	75.3-82.0	66.5-77.6
EDS 6	01 Nov.- 08 Dec. 2000	284	82.2-86.6	63.4-67.5
EDS 8	01 Nov.- 31 Dec. 2002	526	76.0-83.7	60.7-73.5
EDS 9	01 Jan. - 21 Mar. 2003	650	70.9-75.9	73.6-84.4

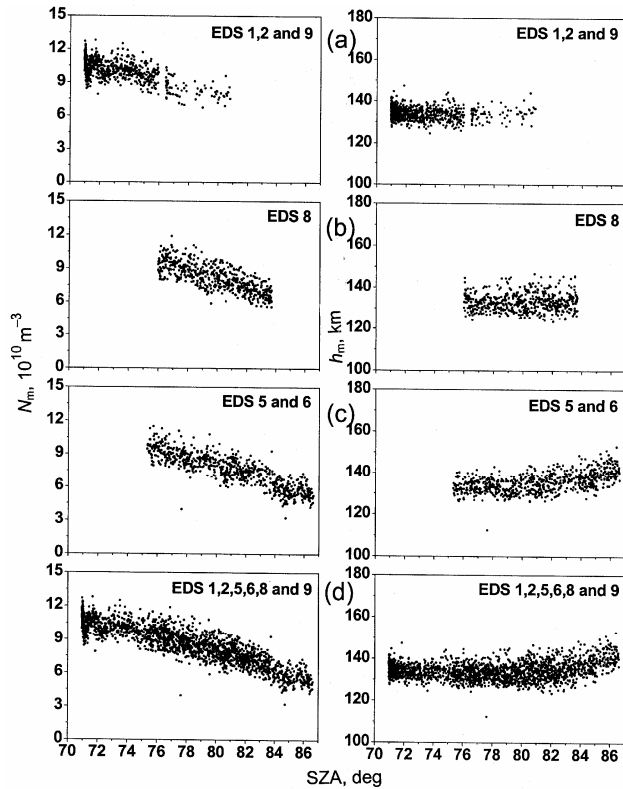


Fig. 3—Demonstrating the response of peak parameters N_m and h_m to solar zenith angle for the near terminator ionosphere

where N_0 is the peak electron density for overhead sun ($\chi = 0$).

It has often been mentioned in the past that the actual electron density profiles at Mars are not expected to be idealized Chapman profiles for a variety of reasons. Firstly Chapman ion layer is produced by photo-ionization of a single molecular species and the molecular ion produced is destroyed locally by dissociative recombination. Secondly, the production of Chapman layer is by monochromatic radiation in an isothermal atmosphere. None of the above two assumptions are truly valid. Electrons are produced by photo-ionization of different neutral particles over a large wave length range, from X-rays to EUV regions. Dissociative recombination of molecular ions is electron temperature dependent, while the Chapman theory assumes an equality between electron, ion and neutral temperatures. Further the region where the maximum ion production and thus the maximum electron density occurs is not isothermal. The neutral temperature increases with altitude from the mesopause to the middle thermosphere and the real isothermality occurs much above the region of maximum ion production. Further

the electron temperature starts departing sharply from the ion and neutral temperature near and above the ion peak³¹, thus questioning the constancy of the dissociative recombination coefficient. In view of the above stated facts, it has been the usual practice in the past to find out how close the Mars primary layer is to Chapman distribution. In other words how close the value of exponent k is to 0.5 in the equation

$$N_m = N_0 (\cos \chi)^k \quad \dots (2)$$

Hantsch and Bauer⁹ obtained a value of 0.57 for k and $2 \times 10^{11} \text{m}^{-3}$ for N_0 by using radio science data from Mariner 4, 6, 7, 9; Mars 2, 4, 6; Viking Orbiter 1, 2 and Viking Lander 1, 2. These data were distributed over different solar activity conditions – from solar minimum to solar maximum over a ten year period.

In a recent attempt, which employed the MGS data, Fox and Yeager³² divided MGS data into various solar activity zones by translating the daily F10.7 values, as observed at Earth to Mars and obtained values 0.42, 0.456 and 0.49 for low, medium and high solar activity conditions. These authors, in addition, obtained values of N_0 as $1.68 \times 10^{11} \text{m}^{-3}$, $1.82 \times 10^{11} \text{m}^{-3}$ and $2.0 \times 10^{11} \text{m}^{-3}$ for low, medium and high solar activity conditions, respectively. In all these cases, a median profile for each day of observations was used. A similar attempt has been made in this paper by analyzing all the observed profiles on each day. This procedure is in contrast to Fox and Yeager who used one median profile for each day. Figures 4(a)-(c) show $N_m \cos \chi$ plots for three sets of data, (1) EDS 1, 2, 9, (2) EDS 8 and (3) EDS 5, 6, thus categorizing these measurements into moderate, moderately high and high solar activity, with the average EUV flux as $2.25 \times 10^{10} \text{cm}^{-2} \text{s}^{-1}$, $2.5 \times 10^{10} \text{cm}^{-2} \text{s}^{-1}$ and $2.75 \times 10^{10} \text{cm}^{-2} \text{s}^{-1}$, respectively for these periods. It needs to be pointed out that MGS data for solar minimum has not been analysed by any group yet. The value of k and N_0 obtained for these periods are given Table 2. These values however, should be treated with caution, since the excursions in χ are rather limited for EDS 1, 2, 9, as well as for EDS 8. To obtain representative values of k and N_0 for the MGS data analysed in this paper, a mass plot of $N_m \cos \chi$ has been generated in Fig. 4(d). Values so derived are again in Table 2 along with those obtained by Hantsch and Bauer⁹ and Fox and Yeager³². It is to be noted that in this paper the same data, as employed by Fox and Yeager were used. These authors divided the data into three solar activity

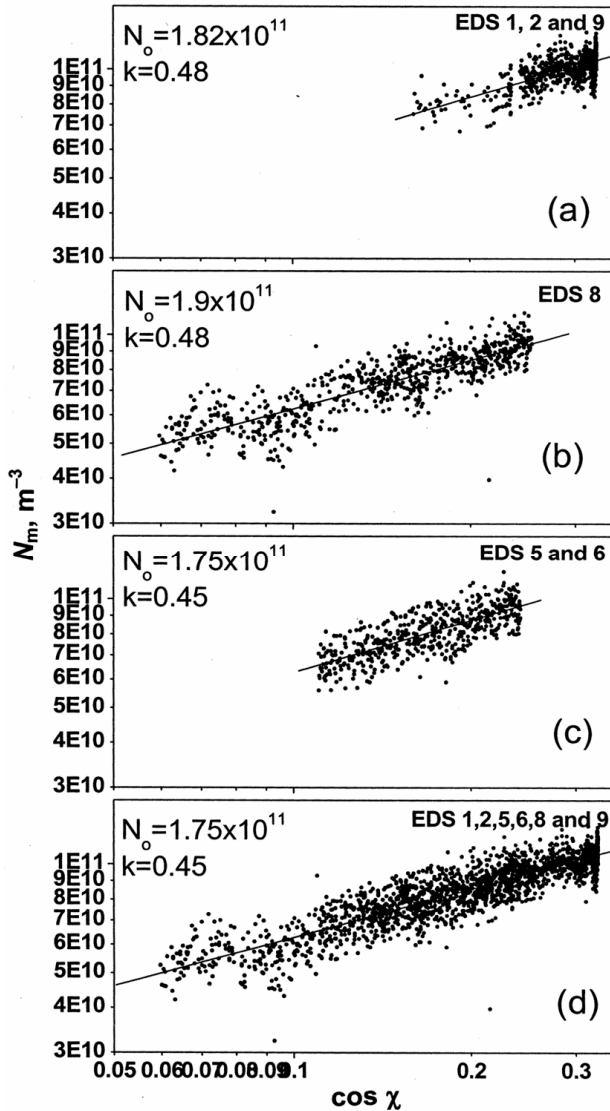


Fig. 4— N_m - $\cos \chi$ plots for various levels of solar EUV flux during sun spot cycle 23 (a)-(c) [Plot in (d) contains all the data from the EDS 1, 2, 5, 6, 8 and 9. These plots are generated to deduce value of exponent k and peak density N_0 for an over-head sun.]

zones based upon the F10.7 solar radio flux, which can show large excursion even during a single solar rotation. On the other hand, the classification made in this paper is on the basis of observed values of EUV flux – the actual parameter responsible for ionization in a planetary ionosphere.

4.3 Anomalous features

As stated earlier, solar zenith angle is an important parameter in determining the height and density of the ionospheric peak for a photochemical layer. The higher the slant angle χ , higher is the altitude of unit optical depth and lower the rate of ion production. The MGS radio science measurements taken on any one day were at a constant SZA and thus it was expected that h_m and N_m would be the same for all the profiles observed on any one day. However, Mahajan *et al.*¹⁷ noted from an analysis of EDS 1, 2, 5 and 6 data sets that h_m and N_m varied considerably on the same day. As stated earlier, variability in h_m had also been noted by Bougher *et al.*¹⁴. They had linked this variability to atmospheric dynamics, operating in response to migrating and non-migrating tidal variations in the lower atmosphere. Mahajan *et al.*¹⁷ had characterized these variability in h_m and N_m as anomalous features of the Martian ionosphere.

With a large number of electron density profiles available from the data sets EDS 8 and EDS 9, it was felt necessary to verify whether the anomalous features seen in N_m and h_m were present in these data sets also. An examination of these profiles indicated that these anomalies were present in these data sets too. This is demonstrated in Fig. 5, which shows five selected profiles out of 12 observed on 09 Feb. 2003. It can be noted that N_m varied between $9.1 \times 10^{10} \text{ m}^{-3}$ and $1.1 \times 10^{11} \text{ m}^{-3}$ while h_m varied between 131.5 and 137.2 km. Longitudinal plots of h_m and N_m for some

Table 2— Values of k and N_0 from major studies

S. No.	Authors	Solar activity	k	$N_0 \times 10^{11}, \text{ m}^{-3}$	Remarks
1	Hantsch and Bauer ⁹	Data for low, moderate and high activity	0.57	2.0	About 90 data points $\chi \approx 50$ -95
2	Fox and Yeager ³²	F10.7: 102-140, flux units	0.42	1.68	About 25 data points $\chi \approx 71$ to 84
3	Fox and Yeager ³²	F10.7: 140-190, flux units	0.47	1.82	About 141 data points $\chi \approx 72$ to 87
4	Fox and Yeager ³²	F10.7: 190-273, flux units	0.49	2.0	About 20 data points $\chi \approx 71$ to 87
5	Kumar <i>et al.</i> (this paper)	EUV flux: $2.25 \times 10^{10}, \text{ cm}^2 \text{ s}^{-1}$	0.48	1.82	725 data points $\chi \approx 71$ to 81
6	Kumar <i>et al.</i> (this paper)	EUV flux: $2.5 \times 10^{10}, \text{ cm}^2 \text{ s}^{-1}$	0.48	1.90	526 data points $\chi \approx 76$ to 84
7	Kumar <i>et al.</i> (this paper)	EUV flux: $2.75 \times 10^{10}, \text{ cm}^2 \text{ s}^{-1}$	0.45	1.75	732 data points $\chi \approx 75$ to 87
8	Kumar <i>et al.</i> (this paper)	EUV flux: 2.25 - $2.75 \times 10^{10}, \text{ cm}^2 \text{ s}^{-1}$	0.45	1.75	1983 data points $\chi \approx 71$ to 87

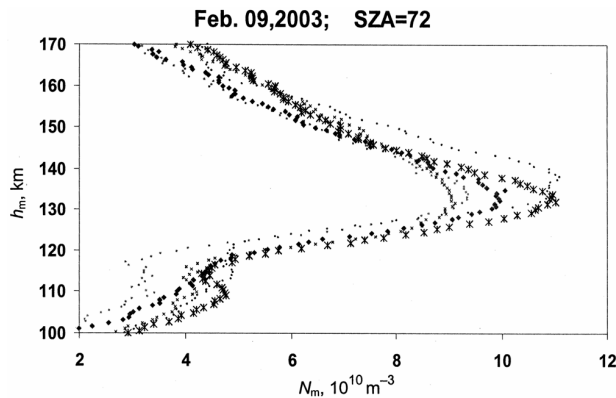


Fig. 5—Demonstrating the variability in the peak parameters h_m and N_m for the same solar zenith angle [This variability is not expected for a photochemical layer and is an anomalous feature of the Martian ionosphere.]

profiles showed the presence of waves, while others did not show any definitive pattern. This feature is being examined in more details for future work.

5 Discussion

A large body of data on electron density profiles at Mars is now available and a lot of new results have come out from the initial analysis of these data sets^{8–10, 12–21, 27–29}. Although solar activity varied considerably during the sunspot cycle 23, the data sets analysed in this paper and by several other workers are basically from a moderate to high solar activity period with the average solar EUV flux values integrated for the wavelength range 26–34 nm varying between 2.25×10^{10} and $2.75 \times 10^{10} \text{ cm}^{-2} \text{ s}^{-1}$. The EUV flux during the minimum of sunspot cycle 23 is a little more than $1 \times 10^{10} \text{ cm}^{-2} \text{ s}^{-1}$, as can be seen in Fig. 2. So the MGS data sets analysed in this paper and by other workers have not been able to provide any definitive results on the Martian ionosphere during solar minimum. However, the excursions in the solar zenith angle χ have been rather quite adequate to examine the χ related changes in h_m and N_m . The values of the exponent k and of the peak electron density for the overhead sun ($\chi = 0$) obtained in this paper are based upon some 2000 profiles and are good representative of a moderately high solar activity period.

The variability in h_m and N_m on the same day and for the same solar zenith angle reported by Mahajan *et al.* by using the data sets EDS 1, EDS 2, EDS 5 and EDS 6, is also seen in the latest data sets, EDS 8 and EDS 9, analysed in this paper. This variability is not expected for a layer in photochemical equilibrium. While the variability in h_m has been attempted to be

explained by Bougher *et al.*^{14,16} on the basis of thermospheric dynamics in response migrating and non-migrating tides in the lower atmosphere, the variability in N_m is difficult to explain. A parameter which might change N_m through its control on the dissociative recombination coefficient is the electron temperature, for which no measurements are available. The next question which comes to one's mind is what could change electron temperature when the solar ionizing flux has remained the same. Could it again be the atmospheric dynamics, which would change the level of constant pressure and thus the value of h_m ? And the modified value of h_m might affect the electron temperature due to its possible dependence on the altitude. There are several such questions which need to be answered in the area of Mars aeronomy, which would be possible when a mission like Pioneer Venus (PV)³³ is attempted on Mars too. The PV mission had almost all the experiments needed for a complete study of a planetary ionosphere.

6 Conclusions

Analysis of some 2000 electron density profiles observed by the radio science experiments on MGS has shown a very definitive and improved relationship of the height and density of the main ionospheric layer on the solar zenith angle. Some anomalous features like the variability in these peak parameters on the same day for the same solar zenith angle are present in all the MGS data sets. These features could be a major area of work in Mars aeronomy.

Acknowledgements

Financial support for this work was provided by the Department of Space, Govt. of India under the PLANEX programme operated by the Physical Research Laboratory, Ahmedabad. The authors Ashok Kumar was Research Associate and Neelesh Kumar Lodhi a Project Assistant during the progress of the PLANEX programme. The authors are thankful to the MGS radio science team for making the Mars electron density data sets available on the public website. They are also thankful to the SOHO/SEM team for making the EUV flux data available on the website. Comments by the reviewers were of great help in improving the presentation of this paper. K K Mahajan is thankful to the Indian National Science Academy for the award of INSA Senior Scientist Scheme.

References

- 1 Kliore A J, Cain D L, Levy G S, Eshelman V R, Fjeldbo G & Drake F D, Occultation experiment: results of the first direct measurement of Mars atmosphere and ionosphere, *Science (USA)*, 149 (1965) 1243.
- 2 Fjeldbo G, Fjeldbo G C & Eshelman V R, Models for the atmosphere of Mars based on the Mariner 4 occultation experiment, *J Geophys Res (USA)*, 71 (1966) 2307.
- 3 Rasool S I & Stewart R W, Results and interpretation of the S-band occultation experiments on Mars and Venus, *J Atmos Sci (USA)*, 28 (1971) 869.
- 4 Kliore A J, Cain D L, Fjeldbo G, Seidel B L, Sykes M J & Rasool S I, The atmosphere of Mars from Mariner 9 radio occultation measurements. *Icarus (USA)*, 17 (1972) 484.
- 5 Kliore A J, Fjeldbo G, Seidel B L, Sykes M J & Woiceshyn P M, S band radio occultation measurements of the atmosphere and topography of Mars with Mariner 9: extended mission coverage of polar and intermediate latitudes. *J Geophys Res (USA)*, 17 (1973) 484.
- 6 Kolosov M A, Yakovlev O I, Kruglov Y M, Trusov B P, Effimov A I & Kerzhanovich V V, Preliminary results of radio occultation studies of Mars by means of the Orbiter Mars-2. *Dokl. Akad. Nauk SSSR (USSR)*, 206 (1972) 1071.
- 7 Hanson W B, Sanatani S & Zuccaro D R, The Martian ionosphere as observed by the Viking retarding potential analyzers, *J Geophys Res (USA)*, 82 (1977) 4351.
- 8 Mendillo M, Withers P, Hinson D, Rishbeth H & Reinisch B, Effects of Solar Flares on the Ionosphere of Mars, *Science (USA)*, 311 (2006) 1135.
- 9 Hantsch M H & Bauer S J, Solar control of the Mars ionosphere, *Planet Space Sci (GB)*, 38 (1990) 539.
- 10 Zhang M H G, Luhmann J G, Kliore A J & Kim J, A post Pioneer Venus reassessment of the Martian dayside ionosphere as observed by radio occultation methods, *J Geophys Res (USA)*, 95 (1990) 14829.
- 11 Kliore A J, *Radio occultation observations of ionospheres of Mars and Venus in Venus and Mars: Atmosphere, ionospheres, and Solar Wind interactions*, edited by J G Luhmann, M Tatrallyay and O Pepin, *Geophys Monogr Ser (USA)*, 66 (1992) 265.
- 12 Hinson D P, Simpson R A, Twicken J D, Tyler G L & Flasar F M, Initial results from radio occultation measurements with Mars Global Surveyor, *J Geophys Res (USA)*, 104 (1999) 26997.
- 13 Tyler G L, Balmini G, Hinson D P, Sjogren W L, Smith D E, Simpson R A, Asmar S W, Priest P & J D Twicken, Radio science observation with Mars Global Surveyor: Orbit insertion through one Mars year in mapping orbit, *J Geophys Res (USA)*, 106, 23 (2001) 327.
- 14 Bougher S W, Engel S, Hinson D P & Forbes J M, Mars Global Surveyor Radio Science electron density profiles: Neutral atmosphere implications, *Geophys Res Lett (USA)*, 28 (2001) 3091.
- 15 Keating G M & 27 colleagues, The structure of the upper atmosphere of Mars: In-situ Accelerometer measurements from Mars Global Surveyor, *Science (USA)*, 279 (1998) 1672.
- 16 Bougher S W, Engel S, Hinson D P & Murphy J R, MGS Radio Science electron density profiles: Interannual variability and implications for the Martian neutral atmosphere, *J Geophys Res (USA)*, 109 (2004) E03010, doi: 10.1029/2003JE002154.
- 17 Mahajan K K, Singh S, Kumar A, Raghuvanshi S & Haider S A, Mars Global Surveyor radio science electron density profiles: Some anomalous features in the Martian ionosphere, *J Geophys Res (USA)*, 112 (2007) E10006, doi:10.1029/2006JE002876.
- 18 Martinis C, Wilson J K & Mendillo M J, Modelling day-to-day ionospheric variability on Mars, *J Geophys Res (USA)*, 108 (2003) A101383, 10.1029/2003JA009973.
- 19 Mendillo M, Smith S, Wroten J, Rishbeth H & Hinson D, Simultaneous ionospheric variability on Earth and Mars, *J Geophys Res (USA)*, 108 (2003) A121432, 10.1029/2003JA009961.
- 20 Rishbeth H & Mendillo M, Ionospheric layers of Mars and Earth, *Planet Space Sci (GB)*, 52 (2004) 849.
- 21 Krymskii A M, Breus T K, Ness N F, Hinson D P & Bojkov D I, Effect of crustal magnetic fields on the near terminator ionosphere at Mars: Comparison of in situ magnetic field measurements with the data of radio science experiments on board Mars Global Surveyor, *J Geophys Res (USA)*, 108 (2003) A121431, doi: 10.1029/2002JA009662.
- 22 Acuna M H, Connerney J E P, Ness N F, Lin R P, Mitchell D, Carlson C W, McFadden J, Anderson K A, Reme H, Mazelle C, Vignes D, Wasilewski P & Cloutier P, Global distribution of crustal magnetization discovered by the Mars Global Surveyor MAG/ER experiment, *Science (USA)*, 284 (1999) 790.
- 23 Krymskii A M, Ness N F, Crider D H, Breus T K, Acuna M H & Hinson D P, Solar wind interaction with the ionosphere/atmosphere and crustal magnetic fields at Mars: Mars Global Surveyor Magnetometer/Electron Reflectometer, radio science and accelerometer data, *J Geophys Res (USA)*, 109 (2004) A11306, doi: 10.1029/2004JA010420.
- 24 Breus T K, Krymskii A M, Crider D H, Ness N F, Hinson D & Barashyan K K, The effect of the solar radiation in the topside atmosphere /ionosphere of Mars: Mars Global Surveyor observations, *J Geophys Res (USA)*, 109 (2004) A09310, doi:10.1029/2004JA010431.
- 25 Zou H, Wang J-S & Nielsen E, Reevaluating the relationship between the Martian ionospheric peak density and the solar radiation, *J Geophys Res (USA)*, 111 (2006) A07305, doi: 10.1029/2005JA011580.
- 26 Tobiska W K, Woods T, Eparvier F, Viereck R, Floyd L, Bouwer D, Rottman G & White O R, The SOLAR 2000 empirical solar irradiance model and forecast tool, *J Atmos Solar-Terr Phys (GB)*, 62 (2000) 1233.
- 27 Wang J S & Nielsen E, Behavior of the Martian dayside electron density peak during global dust storms, *Planet Space Sci (GB)*, 51 (2003) 329.
- 28 Mendillo M, Withers P, Hinson D, Rishbeth H & Reinisch B, Effects of Solar Flares on the Ionosphere of Mars, *Science (USA)*, 311 (2006) 1135.
- 29 Fox J L, Response of Martian thermosphere/ionosphere to enhanced fluxes of solar soft X-rays, *J Geophys Res (USA)*, 109 (2006) doi:10.1029/2004JA010380. A11310.

- 30 Bauer S J, *Physics of Planetary Ionosphere* (Springer-Verlag, New York), 1973.
- 31 Judge D L, McMullin D R, Ogawa H S, Hovestadt D, Klecker B, Hilchenbach M, Mobius E, Canfield L R, Vest R E, Watts R, Tarrio C, Kuhne M & Wurz P, First solar EUV irradiance obtained from SOHO by the CELIAS/SEM, *Sol Phys (Netherlands)*, 177 (1998) 161.
- 32 Hanson W B, & Mantas G P, Viking electron temperature measurement: Evidence for a magnetic field in the Martian atmosphere, *J. Geophys. Res. (USA)*, 93 (1988) 7538.
- 33 Fox J L & Yeager K E, Morphology of the near-terminator Martian ionosphere: A comparison of models and data, *J Geophys Res (USA)*, 111 (2006) A10309, doi:10.1029/2006JA011697.
- 34 Colin L, The Pioneer-Venus programme, *J Geophys Res (USA)*, 85 (1980) 7575.